Microscopic theory of high-field miniband transport in semiconductor superlattices

1997 J. Phys.: Condens. Matter 9 7403

(http://iopscience.iop.org/0953-8984/9/35/014)

J. Phys.: Condens. Matter **9** (1997) 7403–7418. Printed in the UK PII: S0953-8984(97)84322-6

Microscopic theory of high-field miniband transport in semiconductor superlattices

V V Bryksin† and P Kleinert‡

† Physico-Technical Institute, Politekhnicheskaya 26, 194021 St Petersburg, Russia

‡ Paul-Drude-Institut für Festkörperelektronik, Hausvogteiplatz 5-7, 10117 Berlin, Germany

Received 20 May 1997, in final form 26 June 1997

Abstract. A quantum theory of high-field miniband transport in semiconductor superlattices is developed that is applicable in the electric field range where negative differential conductance appears. The lateral electron distribution function is determined from a quantum kinetic equation, in which intracollisional field effects are included. Scattering on polar optical phonons is taken into account. Unlike the Boltzmann equation approach, our theory reproduces the experimentally detected temperature dependence of the current in both the hopping and band transport regimes. Numerical and analytical results show that at low temperatures the lateral electron distribution function strongly deviates from its equilibrium expression and exhibits sharp edges. For a superlattice with a narrow miniband the existence of electro-phonon resonance effects is predicted. The associated resonant-type current anomalies depend strongly on temperature and are most pronounced at low temperatures.

1. Introduction

In the past few years there has been tremendous interest in the transport properties of semiconductor superlattices (SLs). Their unique behaviour is caused by the very anisotropic band structure due to the formation of minibands parallel to the growth direction, and the existence of both localized and extended carrier states. The narrow wavevector minizone and the narrow energy band allow electrons in a SL to perform many Bloch oscillations before being scattered into other parts of the Brillouin zone. As a consequence of this Bragg scattering on the minizone boundaries, negative differential conductance (NDC) appears once the Bloch frequency $\Omega = eEd/\hbar$ (E is the electric field and d the SL period) is higher than some effective scattering rate $1/\tau_{eff}$. NDC in superlattices is a manifestation of the phenomenon that electrons accelerated perpendicular to the layers might probe the negative-effective-mass region of the miniband. A long time ago this effect was predicted by Esaki and Tsu [1]. Some years before this pioneering work, Bychkov and Dykhne [2] had already pointed out that electrons in narrow-band semiconductors heated by a strong electric field can be described by an energy-independent lateral electronic distribution function. This leads to N-shaped current–voltage characteristics, where initially at low electric fields ($eEd \ll \hbar/\tau_{eff}$) the current increases with increasing electric field and decreases proportionally to $1/E$ in the high-field region ($eEd \gg \hbar/\tau_{eff}$).

At nearly the same time, Bryksin and Firsov [3] demonstrated that NDC with a characteristic $1/E$ dependence of the current is due to Houston oscillations of electrons confined to a region of the order of Δ/eE (Δ is the bandwidth) and their inelastic scattering on optical phonons. In the field region where $eEd \gg \hbar/\tau_{eff}$, the separation between

0953-8984/97/357403+16$19.50

the quantized Wannier–Stark levels is much larger than their broadening, and the electron transport results from phonon-induced hopping between localized oscillator-like states with a characteristic hopping distance. In the electric field region where $eEd \gtrsim \hbar\omega_0$ (where ω_0 is the frequency of optical phonons) the appearance of so-called electro-phonon resonances was predicted [3, 4] giving rise to a nonmonotonic current–voltage dependence. Peculiarities observed in the conductance–voltage characteristics of cubic ZnS films have been identified with such resonant-type anomalies around the Wannier–Stark levels [5, 6]. Strong electro-phonon resonance effects were also expected to appear in zeolites [7–10], which have narrow minibands along all directions of the Brillouin zone.

At that time, the main theoretical and experimental interest focused on narrow-band semiconductors, where the energy dispersion relation is not so strongly anisotropic as in SLs. The current in such structures is nearly independent of temperature. These temperature characteristics are due to the heating of the lateral electron motion [3] described by a transverse electron distribution function $n(\boldsymbol{k}_\perp)$ that does not depend on the wavevector components $\boldsymbol{k}_\perp$ perpendicular to the field direction ($n(\boldsymbol{k}_\perp) \approx$ constant). This result should be contrasted with the situation in SLs, which behave quite differently. The miniband transport in a SL strongly depends on temperature [11–13]. This strong temperature dependence mainly results from the electron distribution function, which describes the field-dependent coupling between longitudinal and transverse degrees of freedom. This indicates that the heating of the lateral electron motion in a SL plays a completely different role to the one it plays in narrow-band semiconductors. For a SL structure it is essential to treat the lateral electron heating carefully in order to reproduce the measured strong temperature dependence of the current. To our knowledge this has not been done till now. Most previous theoretical work relied on the so-called 'mean-energy-gain' method [14–16], where $n(\boldsymbol{k}_\perp)$ is replaced by its equilibrium expression. Other approaches approximately eliminated the lateral distribution function [17]. None of these papers account properly for the lateral electron heating and the related temperature dependence of the current. This observation has motivated our study of high-field miniband transport in a SL by determining the nonequilibrium electron distribution function and the related field and temperature dependence of the current.

Other theoretical papers generalized the early work by Esaki and Tsu [1] by treating Boltzmann's equation in the relaxation time approximation at finite temperatures [18, 19]. This semiclassical description of the miniband transport is in good qualitative agreement with experimental results on GaAs/AlAs SLs with narrow miniband widths [11–13]. However, in these one-dimensional transport models the coupling between vertical and lateral degrees of freedom has not been taken into account. Consequently, the field and temperature dependence of the current factorizes, which is not in accordance with experimental data. It has been demonstrated by Gerhardts [20] that the energy transfer to the lateral motion, which makes the miniband transport effectively a three-dimensional problem, leads to a shift of the current maximum with varying miniband width Δ, which deviates significantly from results of the previously studied one-dimensional models. A similar conclusion has been drawn by Lei, Horing and Cui [21, 22] from a balance equation approach, who also reported satisfying agreement with experimental results.

From the analysis of the experimental data it has been claimed that the semiclassical Boltzmann transport model seems to be adequate for the so-called band transport regime occurring above a characteristic temperature of about 40 K [12, 13]. There is, however, a fundamental limitation of the semiclassical Boltzmann approach—namely the neglect of quantum Wannier–Stark localization (WSL), which has been clearly demonstrated to play an essential role in electro-optical experiments on SLs [23–26]. The semiclassical treatment

becomes apparently insufficient at high electric fields, where the states tend to localize and where the electron distribution function might become strikingly different from its equilibrium form.

In the SL miniband transport two different temperature regimes have been observed [12]. At low temperatures and sufficiently high electric fields the eigenstates of electrons are well localized and electrons diffuse through the crystal by hopping processes. The current increases with increasing temperature as predicted by Calecki, Palmier and Chomette [15], who calculated a hopping current linear in the electric field. Above a characteristic temperature ($\sim$40 K) the eigenfunctions extend over many SL periods and the carrier transport is due to more or less extended states. In this regime the current decreases with increasing temperature. While the semiclassical Boltzmann approach provides a fairly good understanding of the high-temperature transport, there is no microscopic approach which adequately describes both regimes at the same level of sophistication.

In this paper we present a rigorous microscopic theory of narrow miniband transport in SLs under the influence of high electric fields. This approach reproduces the measured temperature dependence of the current over the entire temperature interval. In addition, clear electron–phonon resonance effects are predicted to occur in the current–voltage characteristics of a SL. Our theory complements both former semiclassical treatments of the band transport region and quantum mechanical descriptions of the hopping regime, which did not properly account for the lateral electron heating. We hope that our approach will stimulate further experimental and theoretical research of the Wannier–Stark quantum transport in narrow-miniband semiconductor SLs.

2. Quantum theory of high-field transport

Most previous investigations of the miniband transport employed the semiclassical Boltzmann equation, which is valid in the case of vanishing collision broadening ($\Omega\tau_{eff} \ll 1$). In the opposite limit ($\Omega\tau_{eff} \gg 1$), when the WSL prevails, the carrier transport exhibits qualitatively different features, which significantly deviate from predictions made on the basis of classical Boltzmann theory. In this case current anomalies appear such as an oscillatory field dependence of the current and discontinuities in its derivative $\mathrm{d}j/\mathrm{d}E$ (cf. references [3, 4]). These anomalies are due to quantum corrections to the high-field transport and require a rigorous quantum mechanical treatment. A serious disadvantage of former theoretical studies of this transport regime is the simplified treatment of the nonequilibrium distribution function. Almost all authors neglected the lateral electron heating or described it by an equilibrium distribution function (for a review, see [17]).

Many years ago a convenient and general quantum description of the high-field transport in semiconductors was worked out by Bryksin and Firsov [3, 4] and applied to narrow-band semiconductors. The basic concept proposed in these papers provides a suitable starting point for studying the high-field miniband transport in SLs, too. All of the basic transport equations were derived in these papers, so there is no need to repeat all of the technical details here. The interested reader is referred to the original literature [3, 4].

We focus on electron transport in one narrow miniband at low electron concentration so that the electron gas is nondegenerate and Boltzmann statistics applies. In the NDC regime the miniband current perpendicular to the SL layers is expressed by an effective probability $\widetilde{W}$ describing scattering-induced transitions between Stark ladder states [3, 4]:

$$j_x = \frac{n}{E}\frac{\Omega_0^2}{(2\pi)^6}\int \mathrm{d}^3\boldsymbol{k}\int \mathrm{d}^3\boldsymbol{k}'\; n(\boldsymbol{k}'_\perp)(\varepsilon(\boldsymbol{k}')-\varepsilon(\boldsymbol{k}))\widetilde{W}(\boldsymbol{k}',\boldsymbol{k}). \tag{1}$$

Here n is the carrier density, $\Omega_0 = a^2 d$ the volume of the unit cell, and a the lattice constant parallel to the layers. It is a peculiarity of the representation (1) that the current is expressed by an electron distribution function averaged over k_x-values along the SL axis (i.e. parallel to the field direction): $n(\boldsymbol{k}_\perp) = \sum_{k_x} f(\boldsymbol{k})$. This function takes into account the wavenumber-dependent energy transfer into the lateral directions. It is shown below that the elimination of one degree of freedom (namely the k_x-dependence) considerably simplifies the quantum kinetic equation for the electron distribution function.

For the SL energy dispersion relation $\varepsilon(\boldsymbol{k})$ we use the tight-binding model for the motion in the x-direction. The free-electron motion along the lateral directions is described by an effective mass m^*:

$$\varepsilon(\boldsymbol{k}) = \varepsilon(\boldsymbol{k}_\perp) + \frac{\Delta}{2}(1 - \cos(k_x d)) \qquad \varepsilon(\boldsymbol{k}_\perp) = \frac{\hbar^2 k_\perp^2}{2m^*}. \tag{2}$$

The representation (1) of the current allows a simple physical interpretation to be given. In the limit of extremely rare scattering events ($\Omega\tau_{eff} \gg 1$) there is an electric-field-mediated change of the wavevector $\boldsymbol{k}$ with time t according to $k(t) = k(0) + Ft$ with $F = eE/\hbar$. The resulting drift velocity $v = \mathrm{d}\varepsilon/\mathrm{d}\hbar k$ is periodic in t. Consequently, the electrons perform an oscillatory motion with frequency Ω, so on average over time the current vanishes. Scattering events give rise to a change of the electron mean positions, and the carriers jump from layer to layer along the field direction. The related current is due to scattering-induced transitions between Stark levels. Expressions for the effective transition probability $\widetilde{W}$ and the lateral distribution function $n(\boldsymbol{k}_\perp)$ entering this simple picture can only be derived from a rigorous quantum mechanical treatment.

Starting from a quantum kinetic equation for the density matrix and imposing periodic boundary conditions for the distribution function along the k_x-direction, the following general integral equation for the lateral distribution function $n(\boldsymbol{k}_\perp)$ was derived in [3]:

$$\int \mathrm{d}^3\boldsymbol{k}' \int \mathrm{d}k_x \ \left[n(\boldsymbol{k}'_\perp)\widetilde{W}(\boldsymbol{k}', \boldsymbol{k}) - n(\boldsymbol{k}_\perp)\widetilde{W}(\boldsymbol{k}, \boldsymbol{k}')\right] = 0. \tag{3}$$

Solving this equation is a formidable task because the effective scattering rate $\widetilde{W}$ itself satisfies a complicated integral equation [3]. However, if the electric field and the scattering time satisfy the condition $\Omega\tau_{eff} > 1$, the function $\widetilde{W}$ can be expanded in powers of $1/\Omega\tau_{eff}$. In this case it is a good approximation to retain only the first term in this expansion. We will focus on this situation and restrict our consideration to the electron–phonon scattering, where the first term of this series is given [3] by

$$W(\boldsymbol{k}', \boldsymbol{k}) = 2\,\mathrm{Re}\int_0^\infty \mathrm{d}t\ \mathrm{e}^{-st} \sum_{\boldsymbol{q}} \omega_{\boldsymbol{q}}^2 |\gamma_{\boldsymbol{q}}|^2 \left[(N_{\boldsymbol{q}} + 1)\mathrm{e}^{-\mathrm{i}\omega_{\boldsymbol{q}} t} + N_{\boldsymbol{q}}\mathrm{e}^{\mathrm{i}\omega_{\boldsymbol{q}} t}\right]$$
$$\times\ \delta_{\boldsymbol{k}', \boldsymbol{k}+\boldsymbol{q}-\boldsymbol{F}t} \exp\left\{\frac{\mathrm{i}}{\hbar}\int_{-t/2}^{t/2} \mathrm{d}\tau\ \left[\varepsilon(\boldsymbol{k} + \boldsymbol{q} - \boldsymbol{F}\tau) - \varepsilon(\boldsymbol{k} - \boldsymbol{F}\tau)\right]\right\}. \tag{4}$$

Here $\gamma_{\boldsymbol{q}}$ is the matrix element of the electron–phonon coupling, $\omega_{\boldsymbol{q}}$ the phonon frequency, $N_{\boldsymbol{q}} = 1/(\exp(\hbar\omega_{\boldsymbol{q}}/k_B T) - 1)$ the phonon distribution function, and s an adiabatic parameter. The Houston representation (4) of the matrix element W has been derived to lowest order in the electron–phonon coupling and for low carrier concentrations, where correlation effects can be neglected. In the high-field transport regime considered, it is necessary to preserve the explicit field dependence of the transition rate W. A consideration of these intracollisional field effects allows an adequate treatment of the Wannier–Stark localization.

The remaining part of the paper is devoted to the consideration of the particular situation in which electrons are scattered on polar optical phonons with a narrow phonon bandwidth,

which does not mask resonant-type current anomalies resulting from WSL. In addition, to keep our presentation transparent we rely on the simple bulk phonon model, which already reproduces the main qualitative features of the electron–phonon interaction in a SL. In this case the $\boldsymbol{q}$-sum in equation (4) is expressed by an integral ($\sum_{\boldsymbol{q}} \rightarrow (a/2\pi)^3 \int \mathrm{d}^3\boldsymbol{q}$). The exponential term in equation (4) is periodic in q_x ($q_x \rightarrow q_x + 2\pi/d$) and depends on $\boldsymbol{q}_\perp$ only via $\varepsilon(\boldsymbol{k}_\perp + \boldsymbol{q}_\perp)$, so the characteristic transverse electron and phonon momenta are of the same order of magnitude. Denoting the exponential term in equation (4) by $g(\boldsymbol{q})$ and the remaining $\boldsymbol{q}$-dependent factor by $|\gamma_{\boldsymbol{q}}|^2 h(\omega_{\boldsymbol{q}})$, the right-hand side of equation (4) has the following structure:

$$W = \left(\frac{a}{2\pi}\right)^3 \int \mathrm{d}^3\boldsymbol{q}\ |\gamma_{\boldsymbol{q}}|^2 h(\omega_{\boldsymbol{q}}) g(\boldsymbol{q}). \tag{5}$$

Now we neglect the weak $\boldsymbol{q}_\perp$-dependence in $\omega_{\boldsymbol{q}}$ and $\gamma_{\boldsymbol{q}}$, and consider the Fourier representation of $g(\boldsymbol{q})$ with respect to q_x:

$$\begin{aligned} W &= \left(\frac{a}{2\pi}\right)^3 \int \mathrm{d}^2\boldsymbol{q}_\perp \int_{-\infty}^{\infty} \mathrm{d}q_x\ |\gamma_{q_x}|^2 h(\omega_{q_x}) \sum_{l=-\infty}^{\infty} g_l(\boldsymbol{q}_\perp) \mathrm{e}^{\mathrm{i}lq_x d/2\pi} \\ &= \left(\frac{a}{2\pi}\right)^3 \int \mathrm{d}^2\boldsymbol{q}_\perp \int_0^{2\pi/d} \mathrm{d}q_x \sum_{n=-\infty}^{\infty} |\gamma_{q_x+2\pi n/d}|^2 h(\omega_{q_x+2\pi n/d}) \\ &\quad \times \sum_{l=-\infty}^{\infty} g_l(\boldsymbol{q}_\perp) \mathrm{e}^{\mathrm{i}lq_x d/2\pi}. \end{aligned} \tag{6}$$

Here the $g_l(\boldsymbol{q}_\perp)$ are the Fourier coefficients of $g(\boldsymbol{q})$. In the restricted q_x-interval ($0 \leqslant q_x \leqslant 2\pi/d$) the factor $|\gamma_{q_x+2\pi n/d}|^2 h(\omega_{q_x+2\pi n/d})$ depends only weakly on q_x, so the $l = 0$ term dominates the l-sum and we obtain

$$W \cong \left(\frac{a}{2\pi}\right)^3 \int \mathrm{d}^3\boldsymbol{q}\ |\gamma_{q_x}|^2 h(\omega_{q_x})\, g_{l=0}(\boldsymbol{q}_\perp). \tag{7}$$

Making use of the representation

$$g_{l=0}(\boldsymbol{q}_\perp) \frac{d}{2\pi} \int_0^{2\pi/d} \mathrm{d}q_x\ \ g(q_x, \boldsymbol{q}_\perp) \tag{8}$$

and considering only dispersionless optical phonons ($\omega_{q_x} \rightarrow \omega_0$) we arrive at the following expression for the transition probability:

$$\begin{aligned} W(\boldsymbol{k}', \boldsymbol{k}) &= 2\Gamma\omega_0^2\, \mathrm{Re} \int_0^{\infty} \mathrm{d}t\ \mathrm{e}^{-st} \left[(N_0+1)\mathrm{e}^{-\mathrm{i}\omega_0 t} + N_0 \mathrm{e}^{\mathrm{i}\omega_0 t}\right] \\ &\quad \times \int \mathrm{d}^2\boldsymbol{q}_\perp \int_0^{2\pi/d} \mathrm{d}q_x\ \ \exp\left\{\frac{\mathrm{i}}{\hbar} \int_{-t/2}^{t/2} \mathrm{d}\tau\ \ [\varepsilon(\boldsymbol{k} + \boldsymbol{q} - \boldsymbol{F}\tau) - \varepsilon(\boldsymbol{k} - \boldsymbol{F}\tau)]\right\} \\ &\quad \times \delta(\boldsymbol{k}' - \boldsymbol{k} - \boldsymbol{q} + \boldsymbol{F}t) \end{aligned} \tag{9}$$

where

$$\Gamma = \frac{a}{2\pi} \int_0^{2\pi/a} \mathrm{d}q_x\ |\gamma_{q_x}|^2 \tag{10}$$

is an average of the electron–phonon coupling constant along the field direction. As the q-integration has been extended over the entire momentum space, the lattice constant a enters this average and not the SL period d.

For nonpolar optical phonons the approximate replacement of the q-dependent coupling matrix element by a constant Γ is in general use. However, for the Fröhlich coupling of

electrons to polar optical phonons, the q_x-integral in equation (10) should be calculated with caution. In this case finite results are only obtained when the bare coupling constant γ_{q_x} in equation (10) is replaced by its screened value, which prevents the divergence of the q_x-integral. Despite this difficulty, it seems to be necessary to take into account the full q-dependence of the matrix element, when one is interested in reliable quantitative results for the current density. This would prevent the above-mentioned convergence problems from arising but requires further numerical studies.

We will employ equation (9) to calculate the current density from (1). The energy difference $|\varepsilon(\boldsymbol{k}') - \varepsilon(\boldsymbol{k})|$ is approximately given by $\hbar\omega_0$. Due to the underlying spherical symmetry in the y, z-plane, $n(\boldsymbol{k}_\perp)$ depends on $\boldsymbol{k}_\perp$ only via $\varepsilon(\boldsymbol{k}_\perp)$. Inserting equation (9) into (1), the elementary integrals over k_x, k_x' and τ are easily calculated. The remaining $\boldsymbol{k}_\perp$-, $\boldsymbol{k}_\perp'$-integrals are replaced by integrations over the energy parameters ε, ε' with the help of the area density of states

$$\rho_\perp(\varepsilon) = \frac{1}{(2\pi)^2}\int \mathrm{d}^2\boldsymbol{k}_\perp\ \delta(\varepsilon - \varepsilon(\boldsymbol{k}_\perp)) = \frac{m^*}{2\pi\hbar}\Theta(\varepsilon). \tag{11}$$

Putting all of this together, we finally obtain for the current density the explicit expression

$$j_x = \frac{n}{E}\frac{2\Gamma a^4\hbar\omega_0^3}{1-\exp(-\beta)}\int_{-\infty}^{\infty}\mathrm{d}\varepsilon\ \mathrm{d}\varepsilon'\ \rho_\perp(\varepsilon)\rho_\perp(\varepsilon')n(\varepsilon')\left[I_-(\varepsilon',\varepsilon) - \mathrm{e}^{-\beta}I_+(\varepsilon',\varepsilon)\right] \tag{12}$$

with

$$I_\pm(\varepsilon',\varepsilon) = \mathrm{Re}\int_0^\infty \mathrm{d}t\ \mathrm{e}^{-st}G(t)\exp\left[\frac{\mathrm{i}}{\hbar}(\varepsilon' - \varepsilon \pm \hbar\omega_0)t\right] \tag{13}$$

where $\beta = \hbar\omega_0/k_BT$ is the temperature parameter. $G(t)$ is a periodic field-dependent function ($G(t + 2\pi/\Omega) = G(t)$) defined by

$$G(t) = J_0\left(\frac{\Delta}{\hbar\Omega}\sin\left(\frac{\Omega t}{2}\right)\right)^2 \tag{14}$$

and J_0 is the Bessel function. It is convenient to introduce the Fourier transformation of $G(t)$:

$$G(t) = \sum_{l=-\infty}^{\infty}\mathrm{e}^{-\mathrm{i}l\Omega t}\frac{\Omega}{2\pi}\int_{-\pi/\Omega}^{\pi/\Omega}\mathrm{d}t'\ \mathrm{e}^{\mathrm{i}l\Omega t'}G(t') \tag{15}$$

which allows us to carry out the t-integration in equation (13). In the limit $s \to +0$ the quantity $I_\pm$ is expressed by a series of δ-functions, so the ε-integral in equation (12) becomes trivial. Inserting (11), (13), (14) and (15) into equation (12) we obtain for the current density along the SL axis

$$j_x = \frac{J}{1-\exp(-\beta)}\sum_{l=-\infty}^{\infty} f_l\left(\frac{\Delta}{\hbar\Omega}\right)\int_0^\infty \mathrm{d}y\ n(y)\left[\Theta\left(y - 1 - \frac{\Omega}{\omega_0}l\right)\right.$$
$$\left. - \mathrm{e}^{-\beta}\Theta\left(y + 1 - \frac{\Omega}{\omega_0}l\right)\right] \tag{16}$$

with $y = \varepsilon'/\hbar\omega_0$. Here $n(y)$ is the normalized lateral electron distribution function ($\int_0^\infty \mathrm{d}y\ n(y) = 1$) and $J = m^*\omega_0^3a^2\Gamma n/E$ is some effective reference current density. In addition, we have introduced the Fourier coefficients

$$f_l(x) = \frac{1}{\pi}\int_0^\pi \mathrm{d}t\ \cos(lt)J_0^2\left(x\sin\frac{t}{2}\right) = \frac{1}{\pi}\int_0^\pi \mathrm{d}t\ J_l^2(x\sin t). \tag{17}$$

The integral equation (3) for the lateral distribution function $n(\boldsymbol{k}_\perp)$ simplifies accordingly. Starting from equations (3) and (9), and performing the same steps as for the calculation of the current, we obtain the difference equation

$$\sum_{l=-\infty}^{\infty} f_l(x)\left\{\Theta\left(x+1+\frac{\Omega}{\omega_0}l\right)\left[n\left(x+1+\frac{\Omega}{\omega_0}l\right)-\mathrm{e}^{-\beta}n(x)\right]\right.$$
$$\left.+\,\Theta\left(x-1+\frac{\Omega}{\omega_0}l\right)\left[\mathrm{e}^{-\beta}n\left(x-1+\frac{\Omega}{\omega_0}l\right)-n(x)\right]\right\}=0 \tag{18}$$

from which $n(x)$ can be calculated (with $x=\varepsilon/\hbar\omega_0$). Together with the normalization condition for $n(x)$, this equation has a unique solution. By eliminating the k_x-dependence of the distribution function $f(\boldsymbol{k})$ and considering spherical symmetry in the plane, we obtained a simple quantum kinetic equation, in which only one degree of freedom remains. Equations (16) and (18) are new basic results that apply to high-field miniband transport in SLs including the NDC region. These equations support the intuitive picture of the high-field transport as a succession of phonon-induced carrier jumps between Wannier–Stark levels. They include intracollisional field effects and properly describe the lateral electron heating via the nonequilibrium distribution function $n(x)$.

3. The quasi-classical limit

In this section we consider the quasi-classical limit when the hopping length is much smaller than the localization length ($eEd \ll \Delta$). In that case $G(t)$ depends only weakly on Ω, so one can neglect its field dependence:

$$G(t)\approx J_0^2\left(\frac{\Delta}{2\hbar}t\right). \tag{19}$$

Making use of this approximation, the t-integral in equation (13) is easily calculated and we obtain for the current density along the field direction

$$j_x=\frac{J}{\mathrm{e}^{\beta}-1}\frac{1}{\pi}\int_0^{\infty}\mathrm{d}x\;\mathrm{d}x'\;n(x')\left[\mathrm{e}^{\beta}H(x'-x-1)-H(x'-x+1)\right] \tag{20}$$

where the dimensionless energy variables $x=\varepsilon/\hbar\omega_0$ and $x'=\varepsilon'/\hbar\omega_0$ have been introduced. The function H is defined by

$$H(x)=\frac{2}{\alpha\pi}K\left(\sqrt{1-\left(\frac{x}{\alpha}\right)^2}\right)\Theta(\alpha-|x|) \tag{21}$$

with K being the complete elliptic integral of the first kind and $\alpha=\Delta/\hbar\omega_0$ the bandwidth parameter. A somewhat simpler representation for j_x can be derived from equation (20) by calculating the x-integral. For $\alpha<1$ it follows that

$$j_x=\frac{J}{\mathrm{e}^{\beta}-1}\left[\int_{1+\alpha}^{\infty}\mathrm{d}x\;n(x)+\int_{1-\alpha}^{1+\alpha}\mathrm{d}x\;n(x)F\left(\frac{1-x}{\alpha}\right)-\mathrm{e}^{-\beta}\right] \tag{22}$$

where we have introduced

$$F(c)=\frac{2}{\pi^2}\int_c^1\mathrm{d}x\;K(\sqrt{1-x^2})=\frac{1}{2}-\frac{x_0}{\pi}-\frac{1}{\pi^2}\int_{x_0}^{\pi-x_0}\mathrm{d}x\;\arcsin\left(\frac{c}{\sin(x)}\right) \tag{23}$$

with $x_0=\arcsin(c)$ and $F(-c)=1-F(c)$.

In the limit of narrow minibands ($\Delta<\hbar\omega_0$) and temperatures satisfying $\hbar\omega_0<k_BT$, the lateral carrier distribution function is approximately given by its equilibrium expression

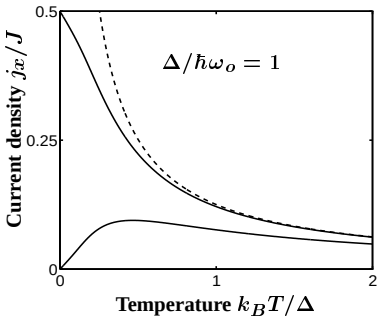

Figure 1. The dimensionless current density j_x/J as a function of the temperature parameter k_BT/Δ for $\Delta/\hbar\omega_0 = 1$. The upper solid line shows the temperature dependence obtained from the Boltzmann equation approach ($j_x/J = I_1(\Delta/2k_BT)/2I_0(\Delta/2k_BT)$, where I_1 and I_0 are modified Bessel functions). The dashed line represents its asymptotic behaviour ($j_x/J = \Delta/8k_BT$). The lower solid line is our result according to equation (27), which behaves asymptotically as $j_x/J = \Delta^2/(8k_BT\hbar\omega_0)$.

$n(x) = \beta\exp(-\beta x)$. In this case some interesting novel analytical results for the current density can be derived from equation (20). To that end, the x'-integral in equation (20) is calculated, which gives

$$j_x = \frac{J}{\mathrm{e}^\beta - 1}\frac{4}{\pi^2}\int_0^1 \mathrm{d}x\ \left[\cosh\left(\frac{\Delta}{k_BT}x\right) - 1\right] K(\sqrt{1-x^2}). \tag{24}$$

The complete elliptic integral K can be replaced by J_0^2 according [27] to

$$K(\sqrt{1-x^2}) = \pi\int_0^\infty \mathrm{d}t\ \cos 2xt\ J_0^2(t). \tag{25}$$

Now we make use of the relationship

$$J_l^2(z) = \frac{1}{\pi}\int_0^\pi \mathrm{d}x\ J_{2l}(2z\sin x) \tag{26}$$

for $l = 0$, which allows us to express the remaining x-integral in equation (24) by the modified Bessel function I_0. Finally, we obtain the following simple analytical result for the current density:

$$j_x = J\left[I_0^2\left(\frac{\Delta}{2k_BT}\right) - 1\right]\Big/\left[\mathrm{e}^\beta - 1\right]. \tag{27}$$

In the limit of high temperatures $\Delta \ll k_BT$ this expression simplifies further and we have

$$j_x = \frac{J}{8}(\Delta/k_BT)^2/\left[\mathrm{e}^\beta - 1\right]. \tag{28}$$

Numerical results for the temperature dependence of the dimensionless current density j_x/J are shown in figure 1 for $\Delta/\hbar\omega_0 = 1$ (lower solid line) and compared with the solution of Boltzmann's equation $I_1(\Delta/2k_BT)/(2I_0(\Delta/2k_BT))$ after reference [19] (upper solid line). Its high-temperature slope $\Delta/(8k_BT)$ is given by the dashed line. At high temperatures ($k_BT > \Delta$) the current density is proportional to $1/T$ ($j_x = J\Delta^2/(8\hbar\omega_0 k_BT)$), which qualitatively agrees with the semiclassical Boltzmann model [18, 19] and experimental results [12, 13]. In the literature it has been claimed that in this high-temperature regime the simple semiclassical description seems to be adequate [12, 13]. At low temperatures ($k_BT < \Delta$) the Boltzmann transport model still predicts an increase of the current with decreasing

temperature, which is in clear contradiction with the experiment [12]. Rather below some crossover temperature the mobility decreases with decreasing temperature, which has been attributed to activated hopping-like transport [12]. The same behaviour is reproduced by our approach (lower solid line), which gives $j_x \sim (k_B T/\Delta)\exp(-(\overline{h}\omega_0 - \Delta)/k_B T)$ in this temperature region. In the quasi-classical limit considered, the decrease of the current density with decreasing temperature is due to the energy conservation law which does not allow one-phonon absorption processes if $\varepsilon < \overline{h}\omega_0 - \Delta$ (and $\Delta < \overline{h}\omega_0$). According to the equilibrium distribution $n(\varepsilon) \sim \exp(-\varepsilon/k_B T)$ the energy of the lateral electron motion vanishes in the limit $T \to 0$, so there is no current if the electric field becomes vanishingly small. We conclude that unlike the semiclassical Boltzmann approach our theory gives a consistent picture of both experimentally distinguished transport regimes, which have been attributed to band transport and hopping conduction, respectively [12].

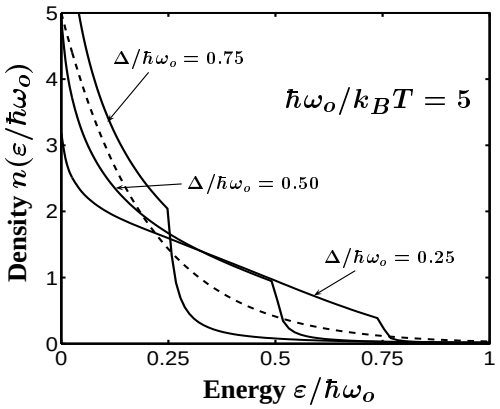

Figure 2. The lateral electron distribution n as a function of the energy parameter $\varepsilon/\overline{h}\omega_0$ for $\overline{h}\omega_0/k_B T = 5$. For the solid lines from bottom to top the parameter $\Delta/\overline{h}\omega_0$ is 0.25, 0.5, and 0.75. The dashed line shows the dependence of the equilibrium distribution $n(x) = \beta\exp(-\beta x)$ on $x = \varepsilon/\overline{h}\omega_0$.

At sufficiently low temperatures the distribution function $n(\varepsilon)$ of the lateral electron motion starts to deviate strongly from its equilibrium expression ($n(\varepsilon) \sim \exp(-\varepsilon)/k_B T$). In this case it is necessary to solve the integral equation (3). Following the same steps of calculation that led to equation (20) we obtain from equations (3) and (9) in the quasi-classical limit (cf. equation (19))

$$\int_0^\infty \mathrm{d}x\ \{n(x)\left[1 + H(x-y-1) + \mathrm{e}^{-\beta}H(x-y+1)\right] - n(y)\left[H(x-y+1) + \mathrm{e}^{-\beta}H(x-y-1)\right]\} = 0. \tag{29}$$

Numerical results for the normalized distribution function calculated from equation (29) are shown in figure 2 for $\overline{h}\omega_0/k_B T = 5$ (solid lines) and compared with $n(x) = \beta\exp(-\beta x)$ (dashed line). From the bottom to the top curves the bandwidth parameter is $\Delta/\overline{h}\omega_0 = 0.25$, 0.5 and 0.75. Each curve deviates remarkably from the equilibrium distribution and exhibits at least one sharp edge at $\varepsilon = \overline{h}\omega_0 - \Delta$.

In the limit of an extremely narrow miniband ($\Delta \ll \overline{h}\omega_0$) the integral equation for the lateral distribution function has the following analytical solution (see the appendix):

$$n(x) = C\mathrm{e}^{-\beta x}\left[1 + \frac{(\alpha\beta)^2}{8}\left(n\coth\left(\frac{\beta}{2}\right) - \frac{\mathrm{e}^{n\beta}}{\cosh\beta - 1}\right)\right] \tag{30}$$

where C is a normalization constant and n an integer defined by $n < x = \varepsilon/\hbar\omega_0 < n+1$. This solution is a stepwise exponential function of the energy variable ε with steps located at multiples of the phonon energy (when the assumed condition ($\alpha \ll 1$) is fulfilled). The analytical solution (30) is only applicable for sufficiently low energy parameters x. Outside this applicability region, $n(x)$ may even become negative.

4. Wannier–Stark quantization

In this section we return to our basic results (equations (16) and (18)) and treat the quantum limit ($\Delta \leqslant eEd$) where the Wannier–Stark localization and the related electron–phonon resonance play a crucial role in understanding the electron transport. First we want to derive some further analytical results for the current density and specialize to the case where $n(x) = \beta \exp(-\beta x)$. Then the y-integral in equation (16) is easily calculated and we obtain immediately

$$j_x = \frac{J}{\mathrm{e}^{\beta}-1}\left\{\sum_{l=1}^{\infty} f_l(\xi)(\mathrm{e}^{-2\gamma l}-1) + \sum_{l=1}^{l_m} f_l(\xi)(\mathrm{e}^{2\gamma l}-1) + \mathrm{e}^{\beta}\sum_{l=l_m+1}^{\infty} f_l(\xi)(1-\mathrm{e}^{-2\gamma l})\right\} \tag{31}$$

where $\xi = \Delta/\hbar\Omega$, $\gamma = \hbar\Omega/2k_BT$ and l_m is the largest integer such that $l_m\Omega/\omega_0 < 1$. In order to further simplify this equation for the current density we take into account equation (26) and

$$\sum_{l=-\infty}^{\infty} \mathrm{e}^{-2l\gamma} J_{2l}(z) = \cosh(z\sinh\gamma). \tag{32}$$

From these equations we obtain

$$\sum_{l=-\infty}^{\infty} f_l(\xi)\mathrm{e}^{-2\gamma l} = I_0^2(\xi\sinh\gamma) \tag{33}$$

which is used to express equation (31) in the form

$$j_x = \frac{J}{\mathrm{e}^{\beta}-1}\left\{I_0^2\left(\frac{\Delta}{\hbar\Omega}\sinh\frac{\hbar\Omega}{2k_BT}\right) - 1 - 4\mathrm{e}^{\beta/2}\sum_{l=l_m+1}^{\infty} f_l\left(\frac{\Delta}{\hbar\Omega}\right)\sinh\frac{\hbar\Omega l}{2k_BT}\sinh\frac{\hbar\Omega l-\hbar\omega_0}{2k_BT}\right\}. \tag{34}$$

The third term on the right-hand side of equation (34) gives rise to a nonmonotonic field dependence of the current and related electro–phonon resonance effects. However, in the limit $\Omega \ll \omega_0$ (or $\hbar\Omega \ll \Delta$) these resonance terms become exponentially small, and the current is given by

$$j_x = J\left[I_0^2\left(\frac{\Delta}{\hbar\Omega}\sinh\frac{\hbar\Omega}{2k_BT}\right) - 1\right] \Big/ \left[\mathrm{e}^{\beta}-1\right]. \tag{35}$$

This result does not exhibit any peculiarities at Wannier–Stark energies and yields a smooth temperature and field dependence of the current density. In the quasi-classical limit ($\Omega \to 0$) equation (35) agrees with equation (27).

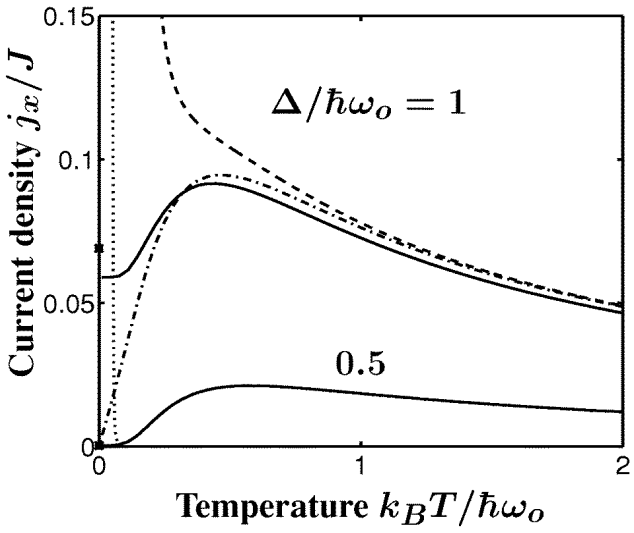

Figure 3. The temperature dependence of the current density j_x/J for $\Delta/\overline{h}\omega_0 = 1$ (upper solid and dashed lines) and $\Delta/\overline{h}\omega_0 = 0.5$ (lower solid and dotted lines). The solid and dashed/dotted lines are calculated from equation (36) and (35), respectively. The chain line shows the quasi-classical result after equation (27) for $\Delta/\overline{h}\omega_0 = 1$.

For extremely low temperatures the l-sum in equation (34) converges only slowly. In this case we find it convenient to use another representation for the current which can be derived directly from equation (31):

$$j_x/J = \sum_{l=l_m+1}^{\infty} f_l(\xi)\left[1 - \exp\left(-\frac{\overline{h}\Omega l}{k_BT}\right)\right] + \frac{2\mathrm{e}^{-\beta}}{1-\mathrm{e}^{-\beta}}\sum_{l=1}^{l_m} f_l(\xi)\left[\cosh\frac{\overline{h}\Omega l}{k_BT} - 1\right]. \tag{36}$$

In the limit of vanishing temperatures ($T \to 0$) and $\Omega \ll \omega_0$ the sums in equation (36) are dominated by contributions around $l = l_m \gg 1$, so we obtain

$$j_x/J \approx f_{l_m+1}(\xi) + f_{l_m}(\xi)\exp\left(\frac{\overline{h}\Omega l_m - \overline{h}\omega_0}{k_BT}\right). \tag{37}$$

When $l_m \gg 1$ we may exploit the asymptotic representation for $f_l(\xi)$ given by

$$f_l(\xi) \approx \frac{1}{2(\pi l)^{3/2}}\exp\left\{-2l\ln\left(\frac{2l}{\xi e}\right)\right\}. \tag{38}$$

This equation can be used to derive the following final result for the current density at zero temperature:

$$j_x/J \approx \frac{1}{\pi(\pi\omega_0/\Omega)^{3/2}}\exp\left[-2\frac{\omega_0}{\Omega}\ln\left(\frac{2}{e}\frac{\overline{h}\omega_0}{\Delta}\right)\right]. \tag{39}$$

In the limit $T \to 0$ the current becomes exponentially small, but remains nonzero. This nonanalytical field dependence of the current ($j_x \sim E^{3/2}\exp(-C/E)$, with C being independent of E) is due to the fact that the energy conservation law is smeared out by the electric field. A similar field dependence appears in the Franz–Keldysh effect for the electroabsorption and in the transport of narrow-band semiconductors [28].

At low temperatures ($k_BT \ll \hbar\omega_0$) and sufficiently high electric fields ($\Delta \ll \hbar\Omega$) again f_{l_m+1} dominates, but this time at $l_m = 0$ ($f_1(\xi) \approx \xi^2/8$), so we obtain from (37)

$$j_x/J \approx \frac{1}{8}\left(\frac{\Delta}{\hbar\Omega}\right)^2. \tag{40}$$

This result simply means that the current becomes essentially temperature independent if eEd is much larger than Δ or $\hbar\omega_0$. Under the influence of such high electric fields the electrons gain enough energy to emit optical phonons independently of the temperature.

Numerical results for the temperature dependence of the current are shown in figure 3 for $\hbar\Omega/\Delta = 0.5$. The solid lines calculated from equation (36) are compared with results obtained from equation (35) (dashed and dotted lines). Above a certain temperature if the bandwidth Δ is smaller than the phonon energy $\hbar\omega_0$ (lower solid line for $\Delta/\hbar\omega_0 = 0.5$) the solid and dotted lines coalesce and agree with the quasi-classical result, equation (27) (not shown in figure 3). The results obtained from equations (35) and (36) for $\Delta/\hbar\omega_0 = 0.5$ strongly deviate from each other only at low temperatures satisfying $k_BT/\hbar\omega_0 \lesssim 0.1$. If Δ becomes comparable with $\hbar\omega_0$ ($\Delta = \hbar\omega_0$), both the semiclassical result (calculated from equation (27), chain line) and the monotonic dependence (obtained from equation (35), dashed line) are no longer a good approximation for the low-temperature behaviour of the current (as calculated from equation (36), upper solid line). Then the nonanalytical dependence of j_x becomes dominant as obtained from equation (39). The $T = 0$ values calculated from equation (39) are marked by asterisks on the ordinate axis in figure 3. Despite this complication, again two different temperature regions can be identified with a crossover temperature of the order of $\hbar\omega_0/k_B$, which is quite similar to the quasi-classical result of section 3.

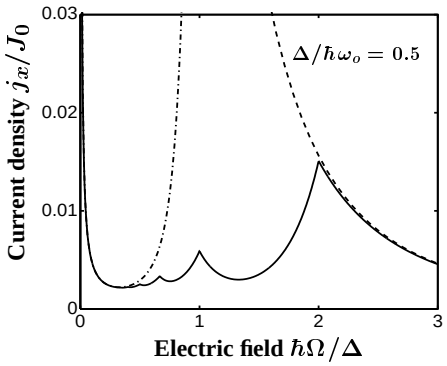

Figure 4. The field dependence of the dimensionless current density j_x/J_0 with $J_0 = enm^*\omega_0^3\Gamma a^2 d/\Delta$ for $\Delta/\hbar\omega_0 = 0.5$ calculated from equation (36) (solid line). Its asymptotic dependence ($j_x/J_0 = (\Delta/2\hbar\Omega)^3$) is shown by the dashed line, and the chain line is obtained from equation (35).

The field dependence of the current as calculated from equation (36) is shown in figure 4 by the solid line and compared with the low-field data (after equation (35), chain line) and the high-field asymptote (after equation (40), dashed line). The curves have been calculated for a low lattice temperature ($\hbar\omega_0 = 10\,k_BT$) and a narrow bandwidth $\Delta/\hbar = 0.5\omega_0$. Pronounced electron–phonon resonant-type anomalies of the current appear at $\hbar\Omega/\Delta = 1/(\alpha n)$ with n being a positive integer. This field dependence of the current is similar to the Shubnikov–de Haas oscillations observed in a two-dimensional electron gas at low transverse magnetic

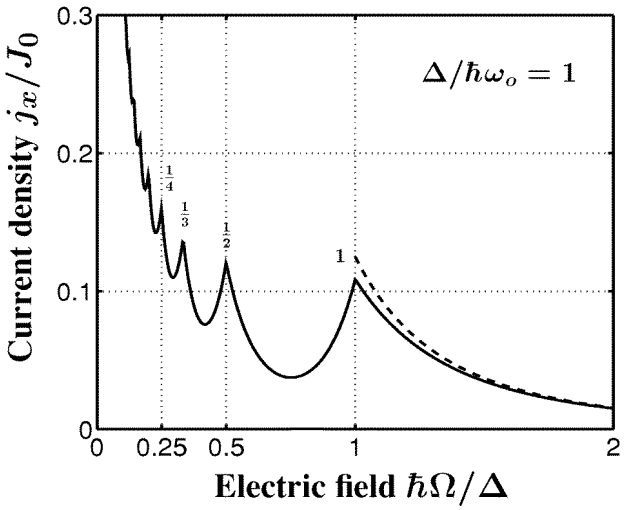

Figure 5. The field dependence of the dimensionless current j_x/J_0 with $J_0 = enm^*\omega_0^3\Gamma a^2 d/\Delta$ for $\Delta/\overline{h}\omega_0 = 1$ as calculated from equation (36) (solid line). Its asymptotic dependence ($j_x/J_0 = (\Delta/2\overline{h}\Omega)^3$) is shown by the dashed line. The current exhibits sharp peaks at $\overline{h}\Omega/\Delta = 1/n$ ($n = 1, 2, \ldots$).

fields. In that case the Landau quantization of the electronic eigenenergies in a magnetic field is responsible for the appearance of oscillations. Another example is shown in figure 5 for $\Delta = \overline{h}\omega_0$ together with its high-field asymptote (dashed line). In this case nonanalytical structures appear at electric field strengths determined by $\overline{h}\Omega = \Delta/n$. In contrast to the case for narrow-band semiconductors [28], these oscillatory current anomalies depend sensitively on temperature and are most pronounced in the low-temperature regime.

Former theoretical treatments [29, 30] of the electron–phonon resonance effects considered only the first term of the perturbation series in powers of the coupling constant. Because this series is divergent as the time tends to infinity one has to sum it, which leads to the kinetic equation (3) for the lateral electron distribution [3]. As shown in section 3 the solution of this equation can deviate significantly from the Boltzmann distribution. Here we derive some analytical results for the distribution function $n(\varepsilon)$ in the limit $\Delta \ll \overline{h}\Omega$ by exploiting the following asymptotic representation:

$$f_l(\xi) \approx \frac{(2l)!}{l!^4}\left(\frac{\xi}{4}\right)^{2l}. \tag{41}$$

In this case $n(\varepsilon)$ can be calculated from equation (18) by considering the fact that the term with $l = 0$ dominates (because $f_l \ll f_0$ if $1 < l$). Retaining only the $l = 0$ contribution, we obtain from equation (18) the solution $n(\varepsilon) \sim \exp(-\beta\varepsilon)$. In order to calculate corrections to this solution we make the *ansatz*

$$n(\varepsilon) = C\mathrm{e}^{-\varepsilon/k_BT}(1 + y(\varepsilon)) \tag{42}$$

and express the energy by $\varepsilon = \overline{\varepsilon} + n\overline{h}\omega_0$ with $0 \leqslant \overline{\varepsilon} \leqslant \overline{h}\omega_0$ and $n = 0, 1, 2, \ldots$. For the small corrections $y(\overline{\varepsilon} + n\overline{h}\omega_0) \equiv y_n$ the following set of recurrence equations is obtained:

$$\begin{aligned} &y_1 - y_0 = \varphi_0 && \text{for } n = 0 \\ &y_{n+1} - y_n + \mathrm{e}^{\beta}(y_{n-1} - y_n) = \varphi_n && \text{for } n \geqslant 1 \end{aligned} \tag{43}$$

where the inhomogeneities are given by

$$\varphi_n = \sum_{l=-\infty}^{\infty} \frac{f_l(\xi)}{f_0(\xi)}(1 - \mathrm{e}^{-2\gamma l})\{\Theta(\overline{\varepsilon} + \overline{\hbar}\omega_0 + (l+n)\overline{\hbar}\Omega) + \mathrm{e}^{\beta}\Theta(\overline{\varepsilon} - \overline{\hbar}\omega_0 + (l+n)\overline{\hbar}\Omega)\}. \tag{44}$$

The set of recurrence equations (43) has the solution

$$y_n = \sum_{m=0}^{n-1} \varphi_m \frac{\mathrm{e}^{(n-m)\beta} - 1}{\mathrm{e}^{\beta} - 1}. \tag{45}$$

Like equation (30), the representation (42) together with the corrections (45) is a stepwise nonanalytical function of the energy variable ε, which is again only applicable if ε is sufficiently small.

5. Conclusion

We presented a microscopic theory for the miniband transport in semiconductor SLs under high electric fields ($eEd > \overline{\hbar}/\tau_{eff}$), where the electronic conduction is governed by hopping-like processes along the field direction aided by emission and absorption of long-wavelength optical phonons. In contrast to the case for systems with confined electronic states, the hopping transport in high electric fields is not activated. This is quite similar to hopping under the influence of strong transverse magnetic fields in a two-dimensional system.

Our main objective in this paper has been to give a clear quantum mechanical picture of the high-field miniband transport in SLs by focusing on the intracollisional field effects and the heating of the lateral electron motion described by a nonequilibrium distribution function. This approach allows us to account for both the so-called band transport and hopping regimes at the same level of sophistication. This is necessary to reproduce the measured temperature dependence of the current. As in the experiment [12], the calculated current density exhibits a maximum at about the Debye temperature $\overline{\hbar}\omega_0/k_B$, which shifts slightly to lower temperatures with increasing bandwidth Δ [12]. At higher temperatures ($\Delta < k_B T$) the current decreases proportionally to $1/T$ with an asymptotic slope $j_x \sim \Delta^2/(k_B T \overline{\hbar}\omega_0)$. This agrees quite well with results of the semiclassical Boltzmann transport model, which has been successfully used to analyse experimental data [13] and which gives a similar asymptotic temperature dependence ($j_x \sim \Delta/k_B T$). Comparing our microscopic approach with the Boltzmann model, the inelastic scattering rate ν_{in} describing relaxation towards an equilibrium distribution [20] can be identified. We find that only parameters of the lateral electron motion enter this scattering rate $\overline{\hbar}\nu_{in} = m^*\omega_0^2 a^2 \Gamma$, where Γ is some averaged electron–phonon coupling constant. According to the Boltzmann approach the current factorizes into a field- and a temperature-dependent part. Here we demonstrated, however, that this factorization is only valid at high temperatures. In general the temperature and field dependencies of the current do not decouple due to the field-mediated coupling between transverse and longitudinal degrees of freedom via the nonequilibrium distribution function. Below the crossover temperature, when the hopping regime dominates, the semiclassical Boltzmann theory predicts a temperature dependence of the current, which even qualitatively deviates from experimental data [12] as well as our theoretical results. In this region the current decreases with decreasing temperature [12]. At $T = 0$ the current reaches a finite value due to the electric-field-induced smearing out of the energy conservation law. Such a peculiarity is also well known from the Franz–Keldysh effect. We conclude that our microscopic approach is the first one which qualitatively reproduces all of the features of

the experimentally detected temperature dependence of the current in the two experimentally distinguished transport regimes.

In the field region $eEd < \hbar\omega_0$ the current is sensitive to temperature as well as changes of the electric field. If the interaction with longitudinal optical phonons is predominant, sharp peaks are expected at $eEd = \hbar\omega_0/n$ ($n = 1, 2, \ldots$) resulting in discontinuities of the differential conductivity. (May and Vecht [6] even observed multiple-phonon resonances at $meEd = n\hbar\omega_0$, with m and n being positive integers.) This resonant-type current anomaly is due to Wannier–Stark localization. When $\hbar\omega_0 < k_B T$ or $\hbar\omega_0 < \Delta$, these oscillations are hardly observable. However, in contrast to the case for narrow-band semiconductors with an isotropic energy dispersion, the electron–phonon resonance effects in SLs depend sensitively on temperature and are most pronounced at low temperatures. Similar anomalies were observed in the conductance–voltage characteristics of cubic ZnS films [6] and identified with the Wannier–Stark effect [29, 30, 5, 6]. Experimental results obtained by Sibille *et al* (see the curve for $\Delta = 4$ meV and $T = 80$ K in their work [13]) could give a first hint that electron–phonon resonance effects are observable in the miniband transport of SLs, too. Further experimental research in this direction is necessary. An adequate theoretical description of the oscillatory current anomalies is complicated by the fact that the lateral electron distribution function may strongly deviate from its equilibrium form, preferentially at low temperatures. This has been clearly demonstrated by the numerical and analytical results presented in this paper.

In comparing our approach quantitatively with experimental data, we must remember that there are other interaction mechanisms such as those with impurities, acoustic phonons and interface roughness scattering, which play an essential role at low temperatures and may broaden the electron–phonon resonance effects due to WSL. Furthermore, we point out that Zener tunnelling between different minibands can play a crucial role in the current–voltage characteristics of the SL transport [17].

Oscillatory current instabilities and the formation of high-field domains due to WSL have been experimentally observed [31, 32] and theoretically analysed [33] for highly doped samples with a sufficiently large charge density, which leads to the formation of a stable field domain boundary. Actually, a spatially homogeneous current distribution such as is considered in the paper at hand appears only at extremely low carrier densities.

Acknowledgments

One of the authors (VVB) would like to acknowledge support by the Russian Foundation of Fundamental Research (Project No 96-02 16848-a). PK acknowledges support from the Deutsche Forschungsanstalt für Luft- und Raumfahrt.

Appendix. Derivation of an analytical expression for the lateral density distribution

In this appendix, analytical results are derived for the lateral electron distribution function $n(x)$ for the case where $\Delta \ll \hbar\omega_0$. We consider the quasi-classical limit in which the influence of an electric field on the scattering probability W can be neglected. In this case the integral equation (3) ($\widetilde{W} \to W$) can be written in a more explicit form:

$$\int_{-\infty}^{\infty} \mathrm{d}\varepsilon\ \rho_\perp(\varepsilon)\{n(\varepsilon)\,[(N_0+1)\delta(\varepsilon-\varsigma-\hbar\omega_0+A)+N_0\delta(\varepsilon-\varsigma+\hbar\omega_0+A)] - n(\varsigma)\,[(N_0+1)\delta(\varepsilon-\varsigma+\hbar\omega_0+A)+N_0\delta(\varepsilon-\varsigma-\hbar\omega_0+A)]\} = 0 \tag{A1}$$

with the abbreviation

$$A = -\frac{\Delta}{2}(\cos k - \cos k'). \tag{A2}$$

Expanding this equation with respect to Δ (or A) and collecting all lowest-order contributions, we obtain the following difference–differential equation for the lateral density distribution:

$$\begin{aligned}\frac{\Delta^2}{8}\rho_\perp(\zeta+\hbar\omega_0)n''(\zeta+\hbar\omega_0) + \frac{\Delta^2}{8}\mathrm{e}^{-\beta}\rho_\perp(\zeta-\hbar\omega_0)n''(\zeta-\hbar\omega_0) \\ + \rho_\perp(\zeta+\hbar\omega_0)n(\zeta+\hbar\omega_0) - n(\zeta)\rho_\perp(\zeta-\hbar\omega_0) \\ + \mathrm{e}^{-\beta}[\rho_\perp(\zeta-\hbar\omega_0)n(\zeta-\hbar\omega_0) - n(\zeta)\rho_\perp(\zeta-\hbar\omega_0)] = 0\end{aligned} \tag{A3}$$

which has the exact analytical solution given by equation (30).

References

[1] Esaki L and Tsu R 1970 *IBM J. Res. Dev.* **14** 61
[2] Bychkov Y A and Dykhne A M 1965 *Zh. Eksp. Teor. Fiz.* **48** 1174 (Engl. Transl. 1965 *Sov. Phys.–JETP* **21** 783)
[3] Bryksin V V and Firsov Y A 1971 *Zh. Eksp. Teor. Fiz.* **61** 2373 (Engl. Transl. 1971 *Sov. Phys.–JETP* **34** 1272)
[4] Bryksin V V and Firsov Y A 1972 *Solid State Commun.* **10** 471
[5] Maekawa S 1970 *Phys. Rev. Lett.* **24** 1175
[6] May D and Vecht A 1975 *J. Phys. C: Solid State Phys.* **8** L505
[7] Bogomolov V N, Zadorozhnyi A I and Pavlova T M 1981 *Fiz. Tekh. Poluprov.* **15** 2029 (Engl. Transl. 1981 *Sov. Phys.–Semicond.* **15** 1176)
[8] Bryksin V V, Firsov Y A and Ktitorov S A 1981 *Solid State Commun.* **39** 385
[9] Bryksin V V 1987 *Fiz. Tverd. Tela* **29** 1141 (Engl. Transl. 1987 *Sov. Phys.–Solid State* **29** 651)
[10] Bryksin V V 1987 *Fiz. Tverd. Tela* **29** 2027 (Engl. Transl. 1987 *Sov. Phys.–Solid State* **29** 1166)
[11] Sibille A, Palmier J F, Wang H and Mollot F 1990 *Phys. Rev. Lett.* **64** 52
[12] Grahn H T, von Klitzing K, Ploog K and Döhler G H 1991 *Phys. Rev.* B **43** 12 094
[13] Sibille A, Palmier J F, Hadjazi M, Wang H, Etemadi G, Dutisseuil E and Mollot F 1993 *Superlatt. Microstruct.* **13** 247
[14] Tsu R and Döhler G 1975 *Phys. Rev.* B **12** 680
[15] Calecki D, Palmier J F and Chomette A 1984 *J. Phys. C: Solid State Phys.* **17** 5017
[16] Geller Y L and Leburton J P 1995 *Phys. Rev.* B **52** 2779
[17] Movaghar B 1987 *Semicond. Sci. Technol.* **2** 185
[18] Shik A Y 1973 *Fiz. Tekh. Poluprov.* **7** 261 (Engl. Transl. 1973 *Sov. Phys.–Semicond.* **7** 187)
[19] Suris R A and Shchamkhalova B S 1984 *Fiz. Tekh. Poluprov.* **18** 1178 (Engl. Transl. 1984 *Sov. Phys.–Semicond.* **18** 738)
[20] Gerhardts R R 1993 *Phys. Rev.* B **48** 9178
[21] Lei X L, Horing N J M and Cui H L 1991 *Phys. Rev. Lett.* **66** 3277
[22] Lei X L, Horing N J M and Cui H L 1992 *J. Phys.: Condens. Matter* **4** 9375
[23] Mendez E E, Rueda F A and Hong J M 1988 *Phys. Rev. Lett.* **60** 2426
[24] Bleuse J, Bastard G and Voisin P 1988 *Phys. Rev. Lett.* **60** 220
[25] Tanaka I, Nakayama M, Nishimura H, Kawashima K and Fujiwara K 1992 *Phys. Rev.* B **46** 7656
[26] Linder N, Schmidt K H, Geisselbrecht W, Döhler G H, Grahn H T, Ploog K and Schneider H 1995 *Phys. Rev.* B **52** 17 352
[27] *Tables of Integrals, Series and Products* 1980 ed I S Gradshteyn and I M Ryzhik (New York: Academic)
[28] Bryksin V V 1972 *Fiz. Tverd. Tela* **14** 802 (Engl. Transl. 1972 *Sov. Phys.–Solid State* **14** 684)
[29] Saitoh M 1972 *J. Phys. C: Solid State Phys.* **5** 914
[30] Sawaki N and Nishinaga T 1977 *J. Phys. C: Solid State Phys.* **10** 5003
[31] Kwock S H, Grahn H T, Ramsteiner M, Ploog K, Prengel F, Wacker A, Schöll E, Murugkar S and Merlin R 1995 *Phys. Rev.* B **51** 9943
[32] Grahn H T, Haug R J, Müller W and Ploog K 1991 *Phys. Rev. Lett.* **67** 1618
[33] Schwarz G and Schöll E 1996 *Phys. Status Solidi* b **194** 351